AGU PUBLICATIONS

JGR

Journal of Geophysical Research: Oceans

RESEARCH ARTICLE

10.1002/2013JC009745

**Key Points:**
- Annual frequency of extreme hot days increased in CUE for 1982–2012
- Extreme hot days excess is lower at the coast than at the ocean
- Difference in extreme hot days (ocean-coast) is strong during upwelling

**Correspondence to:**
M. deCastro,
mdecastro@uvigo.es

**Citation:**
deCastro, M., M. Gómez-Gesteira, X. Costoya, and F. Santos (2014), Upwelling influence on the number of extreme hot SST days along the Canary upwelling ecosystem, *J. Geophys. Res. Oceans*, *119*, 3029–3040, doi:10.1002/2013JC009745.

Received 18 DEC 2013
Accepted 5 MAY 2014
Accepted article online 8 MAY 2014
Published online 22 MAY 2014

# Upwelling influence on the number of extreme hot SST days along the Canary upwelling ecosystem

**M. deCastro[1], M. Gómez-Gesteira[1], X. Costoya[1], and F. Santos[1,2]**

[1]Environmental Physics Laboratory, Universidade de Vigo, Ourense, Spain, [2]Centro de Estudos do Ambiente e do Mar, Physics Department, University of Aveiro, Aveiro, Portugal

**Abstract** Trends in the number of extreme hot days (days with SST anomalies higher than the 95% percentile) were analyzed along the Canary upwelling ecosystem (CUE) over the period 1982–2012 by means of SST data retrieved from NOAA OI1/4 Degree. The analysis will focus on the Atlantic Iberian sector and the Moroccan subregion where upwelling is seasonal (spring and summer) and permanent, respectively. Trends were analyzed both near coast and at the adjacent ocean where the increase in the number of extreme hot days is higher. Changes are clear at annual scale with an increment of $9.8 \pm 0.3$ ($9.7 \pm 0.1$) days dec$^{-1}$ near coast and $11.6 \pm 0.2$ ($13.5 \pm 0.1$) days dec$^{-1}$ at the ocean in the Atlantic Iberian sector (Moroccan subregion). The differences between near shore and ocean trends are especially patent for the months under intense upwelling conditions. During that upwelling season the highest differences in the excess of extreme hot days between coastal and ocean locations ($\Delta$n(# days dec$^{-1}$)) occur at those regions where coastal upwelling increase is high. Actually, $\Delta$n and upwelling trends have shown to be significantly correlated in both areas, $R = 0.88$ ($p < 0.01$) at the Atlantic Iberian sector and $R = 0.67$ ($p < 0.01$) at the Moroccan subregion.

## 1. Introduction

Increase in sea surface temperature (SST) is especially important in coastal areas due to its severe impact in coastal ecosystems [*Honkoop et al*., 1998; *Diederich et al*., 2005; *Burrows et al*., 2011]. Recently, *Lima and Wethey* [2012] detected that during the last three decades ~71.6% of the world coastal locations have experienced a warming trend of $0.25 \pm 0.13$°C dec$^{-1}$ and 6.8% a cooling of $-0.11 \pm 0.10$°C dec$^{-1}$ and that the remaining 22.2% has not undergone any significant variation. They also detected that warming is not homogeneous through the year. In particular, coastal warming occurred mostly in summer along the Southwest European coast. *Cheung et al*. [2013] showed that ocean warming has already affected global fisheries during the last four decades. Marine fishes respond to warming through distribution shifts to higher latitudes and deeper waters.

Apart from changes in mean temperature, the frequency of extreme sea temperatures such as extremely hot or cold events is fundamental to understand changes in coastal marine ecosystems and to determine scenarios and policies to mitigate those changes [i.e., *Philippart et al*., 2003; *Frank et al*., 2005; *Thieltges*, 2006; *Occhipinti-Ambrogi*, 2007]. Thus, the increase (decrease) in the number of extreme hot (cold) days along the Eastern Atlantic margin was also analyzed by *Lima and Wethey* [2012]. Although the study of extreme temperatures over land has been widely discussed in the context of heat waves and its impact on mortality [*Dessai*, 2002; *García-Herrera et al*., 2005; *Díaz et al*., 2006; *Trigo et al*., 2009; *Barriopedro et al*., 2011; *deCastro et al*., 2011], there are very few studies focused on extreme SST events, both near coast and at the ocean, despite their potential effect on marine ecosystems [*Lima et al*., 2006, 2007; *Wethey et al*., 2011].

Coastal upwelling areas are especially important since approximately 20% of the global fish catch occurs in those regions which occupy <1% of the world's ocean [*Pauly and Christensen*, 1995]. Detailed information about the impact of coastal sea warming in the biology of the coastal ecosystems can be seen in *Gómez-Gesteira et al*. [2008a, 2008b, and references therein]. The analysis of extreme hot SST trends in upwelling regions constitutes an important step in developing plans to assess the warming impact on economy and food security of coastal areas.

The Canary upwelling ecosystem (CUE), which extends from 12°N to 43°N, is one of the four major eastern boundary upwelling systems worldwide. According to *Arístegui et al*. [2009], the CUE can be divided into

five subregions attending to their physical environment, shelf dynamics, and circulation. The Atlantic Iberian sector, which includes the west coasts of Galician and Portuguese subregions, is characterized by a seasonal upwelling due to the seasonal change of the zonal component of wind depending on the position of the Azores High. The Gulf of Cadiz subregion represents the major interruption in the continuity of upwelling due to its coastline orientation unfavorable to upwelling. The Moroccan subregion (from 21°N to 33°N) is the only subregion characterized by a permanent upwelling although with seasonal variations. Finally, the Mauritanian-Senegalese is the fifth subregion representing the southern limit of the CUE. In this region, neither permanent nor seasonal upwelling occurs [*Kostianoy and Zatsepin*, 1996].

The analysis of the extreme hot SST events will focus on the Atlantic Iberian sector and the Moroccan subregion where upwelling is a main driving mechanism.

Research recently conducted shows that the Atlantic sector has warmed over the last four decades [*Lemos and Sansó*, 2006; *Gómez-Gesteira et al*., 2008a; *Belkin*, 2009; *Gómez-Gesteira et al*., 2011]. In addition, warming seems to be different at coastal and ocean locations, as pointed out by different authors [*Relvas et al*., 2009; *Santos et al*., 2011a, 2012a], who showed that warming is more intense at ocean locations than at the adjacent coastal locations. *Santos et al*. [2011a] detected a significant near shore (0.28°C $dec^{-1}$) and oceanic (0.30°C $dec^{-1}$) warming along the Western Iberian (WI) coast. *Relvas et al*. [2009] analyzed the same area and also found that warming is more intense at the ocean than near shore, especially during the upwelling season. The same phenomenon was observed at other areas characterized by important fishing banks like the Moroccan subregion [*Santos et al*., 2012c]. In this region, an ocean warming trend of 0.40°C $dec^{-1}$ and a costal warming trend of 0.35°C $dec^{-1}$ were measured over the period 1982–2010. *Santos et al*. [2012b] also analyzed the Benguela Upwelling Ecosystem (BUES) and observed a marked contrast between ocean warming (0.06°C $dec^{-1}$) and coastal cooling (−0.13°C $dec^{-1}$). Both for the CUES and the BUES, the different warming rates at ocean and coastal regions were related to the intensification of upwelling. Previous research dealing with changes in upwelling along the CUE [*Lemos and Pires*, 2004; *McGregor et al*., 2007; *Gómez-Gesteira et al*., 2008b; *Pardo et al*., 2011; *Santos et al*., 2011b; *Gómez-Gesteira et al*., 2011; *Santos et al*., 2012a, 2012c; *Barton et al*., 2013; *Cropper et al*., 2014] have shown a certain controversy due to the high dependence of upwelling trends on the area, the period under study, the season, and even the database. *Lemos and Pires* [2004] concluded that the Portuguese upwelling regime has weakened since the 1940s, being the waning significant throughout the upwelling season (April–September). *McGregor et al*. [2007] found a dramatic SST decrease (related to upwelling increase) in the African upwelling region over the last century. However, their study was based on a proxy derived from the analysis of two cores near Cape Ghir in Morocco and not on SST data sampled in situ. Their results were corroborated by wind observations from COADS that showed wind intensification over the region after 1950. *Gómez-Gesteira et al*. [2008b] show the time evolution of upwelling for the Canary region over the period 1967–2006 (see Figure 9 in their manuscript). Upwelling tends to decrease when considering the whole period for both seasons (under more favorable and less favorable upwelling conditions). Nevertheless, the trend is unclear when considering values from the mid-1980s. These differences between long-term and midterm (a few decades) trends were also pointed out by *Pardo et al*. [2011]. These authors showed that upwelling intensity had decreased along the Iberian/Canary region (see Table A1 in their manuscript). Nevertheless, they considered trends at annual scale, which can be misleading, especially for the Iberian region where upwelling is seasonal. *Santos et al*. [2011a] observed a long-term (1948–2008) decreasing trend for upwelling along the western Iberian coast. The same authors *Santos et al*. [2011b] suggested that trends are far from linear and that quasiperiodic oscillations can affect the signal in such a way that the resulting long-term trend can be positive instead of negative. *Santos et al*. [2012c] found a positive trend for the Canary region over the period 1982–2010. In addition, *Barton et al*. [2013] show that upwelling trends are strongly dependent both on the position of the point and on the data base. In addition, the period under scope is also crucial due to decadal variations. Finally, *Cropper et al*. [2014] also show that the area and the database influence the tendency of upwelling-favorable winds off Northwest Africa (11°N–35°N) during summer (JJA) over the period 1981–2012. They used seven different sources to calculate the $UI^{W}$ in order to compare different observational and reanalysis sources across the selected time period. In fact, trend directions often differ between observational and reanalysis data sets. Observational upwelling indices favor an increase in upwelling across 21°N–35°N and increase in downwelling south of 19°N. Reanalysis-derived upwelling indices support the trend increase across 26°N–35°N but appear mainly monotonic across the lower latitudes.

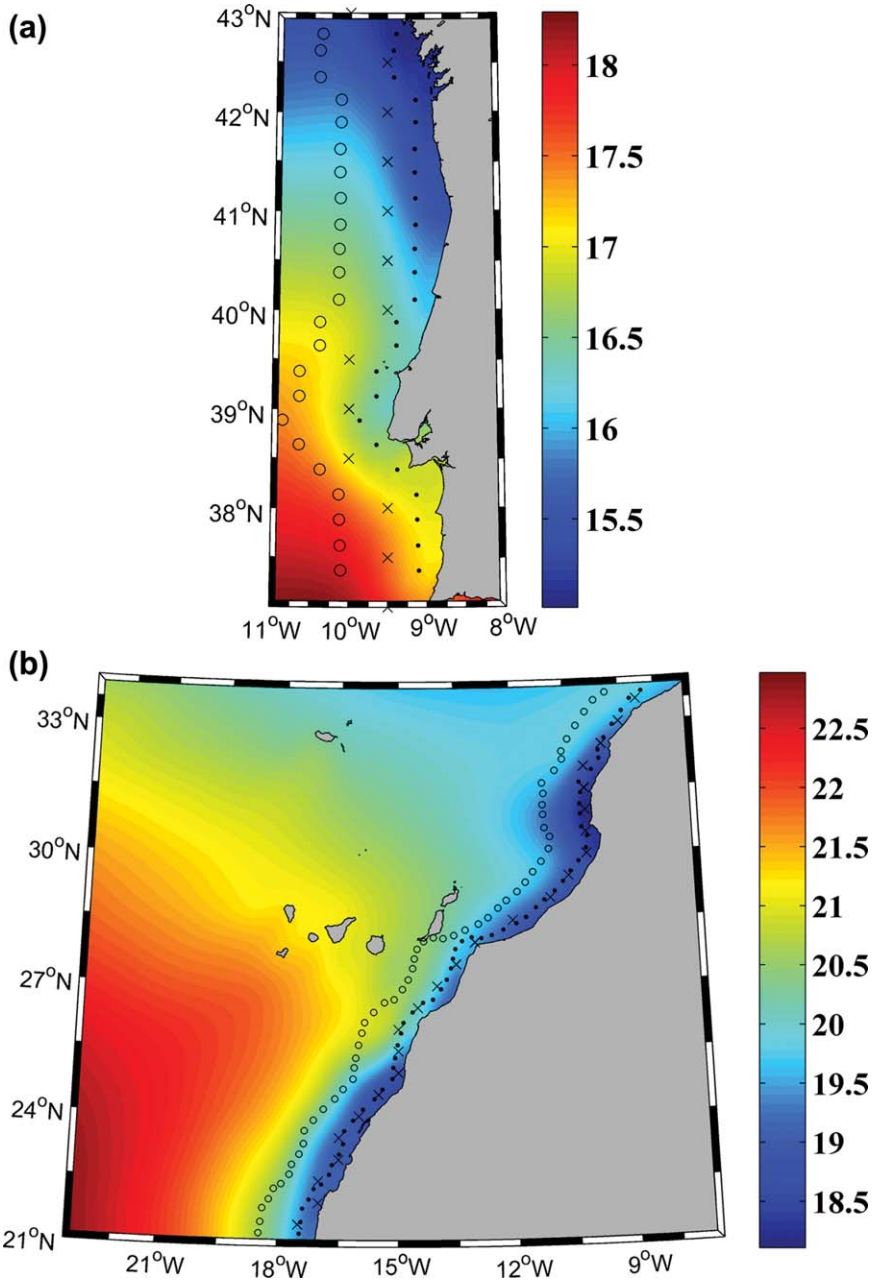


**Figure 1.** (a) Atlantic Iberian sector and (b) Moroccan subregion of the CUE. Colors represent mean SST (°C) averaged from 1982 to 2012. The upwelling imprint is reflected by a seaward SST gradient. Dots (circles) correspond to coastal (ocean) pixels. Crosses represent the locations where upwelling index was calculated.

The question addressed in this paper is the analysis of changes observed in the number of extreme hot days along the Atlantic Iberian sector and the Moroccan subregion of the CUE over the period 1982–2012. In particular, trends will be observed to be different at ocean and coastal locations and we hypothesize that those differences are due to changes in upwelling intensity.

## 2. Area and Data Processing

### 2.1. Area Under Scope

The Atlantic Iberian sector covers the region 37°N–43°N and 8°W–11°W, which corresponds to the West Iberian coast and its adjacent shelf (Figure 1a). The WI coast has an almost constant S-N orientation without

any island, large peninsula or semienclosed basin. The region may be regarded as the northern boundary of the CUES as mentioned above. Previous studies [*Santos et al*., 2005; *Álvarez et al*., 2008] carried out at the WI have shown that coastal upwelling is the most important driving factor during spring and summer. Keeping in mind that positive values of the upwelling index (UI) correspond to favorable upwelling conditions, *Álvarez et al*. [2008] showed that the index is higher than 600 $m^3\ s^{-1}\ km^{-1}$ from April to September, and attains maximum values (around 1000 $m^3\ s^{-1}\ km^{-1}$) from June to August.

The Moroccan subregion covers the region 21°N–34°N and 7°W–23°W which corresponds to the Moroccan and Western Sahara coasts and their adjacent shelf (Figure 1b). As previously mentioned, this region is characterized by a permanent upwelling throughout the year although with seasonal variations [*Arístegui et al*., 2009; *Gómez-Gesteira et al*., 2008a]. *Santos et al*. [2012c] showed that UI is positive all over the year with values higher than 800 $m^3\ s^{-1}\ km^{-1}$ from April to September and maximum values (over 1200 $m^3\ s^{-1}\ km^{-1}$) from June to August.

### 2.2. SST Data

SST values and their associated errors were retrieved from NOAA OI1/4 Degree Daily SST data provided by NOAA's National Climatic data Center. Daily data extend back to 1982 with a spatial resolution of 0.25° × 0.25°. Details of NOAA's OI algorithm and its bias treatment can be found in *Reynolds* [2009] and *Reynolds and Chelton* [2010]. The suitability of the data base to identify extreme events was previously shown in *Lima and Wethey* [2012].

The analysis of coastal SST requires the consideration of pixels very close to land. Only coastal pixels (marked with dots in Figure 1) with <50% of land contamination were considered following the procedure described by *Lima and Wethey* [2012]. Twenty-three ocean points (circles in Figure 1a) were considered for the Atlantic Iberian sector at the same latitude as the coastal ones (dots in Figure 1a) but displaced one degree seaward. The same procedure was followed for the 58 ocean points considered in the Moroccan subregion (circles in Figure 1b).

### 2.3. SST Trends

Warming rates were calculated as the slope of seasonal detrended SST versus time for every pixel individually. Results were expressed in °C $dec^{-1}$. SST OI estimates are affected by errors mainly due to random sampling and bias. The regression procedure accounted for these errors by using weighted least squares, with weights proportional to the inverse of the variance of SST OI. Daily SST values can also be affected by temporal autocorrelation, in such a way that the real degrees of freedom ($N_{eff}$) is much smaller than the sample size (N). The degrees of freedom were calculated using the Quenouille procedure [*Quenouille*, 1952] following *Lima and Wethey* [2012]. In this way, $N_{eff}$ was calculated following $N_{\mathrm{eff}} = N(1-r_1)/(1+r_1)$, where $r_1$ is the lag-1 autocorrelation coefficient of the detrended series. Obviously, $N_{eff}$ will depend on the pixel, but the mean number of degrees of freedom decreased from 11,315 to 373 in the Atlantic Iberian sector and from 11,315 to 498 in the Moroccan subregion.

### 2.4. Extreme SST Trends

The analysis of trends in the number of extreme hot days per decade was carried out for each pixel following several steps: (i) SST anomaly was calculated for each day over the period 1982 to 2012. Anomalies were calculated by removing the seasonal component. This was achieved by subtracting from the temperature of a certain day (e.g., 1 January 1982) the mean temperature of that day (1 January) over the period 1982–2012; (ii) the number of days per year $\left({}^{95}N_{i,j}\right)$ with extremely high SST anomaly (over the 95 percentile) was calculated at annual scale, where *i* and *j* correspond to the longitude and latitude of the pixel and the superscript 95 refers to the percentile; (iii) the annual trends were calculated as the slope of the linear regression of ${}^{95}N_{i,j}$ versus time. This procedure generates a matrix of trends in the number of extreme hot events $\left({}^{95}\Delta N_{i,j}\right)$ and its associated matrix of standard deviations $\left({}^{95}\sigma_{i,j}\right)$. The standard deviation of the trend was calculated following *Press et al*. [1992, section 15.2); (iv) trends at the coastal and ocean points shown in Figure 1 were calculated by spatially averaging the $\left({}^{95}\Delta N_{i,j}\right)$ matrix in the closest neighborhood of every pixel *i*, *j*. The combined standard deviation was calculated considering the standard deviation and mean of the pixels in the neighborhood of pixel *i*, *j* following:

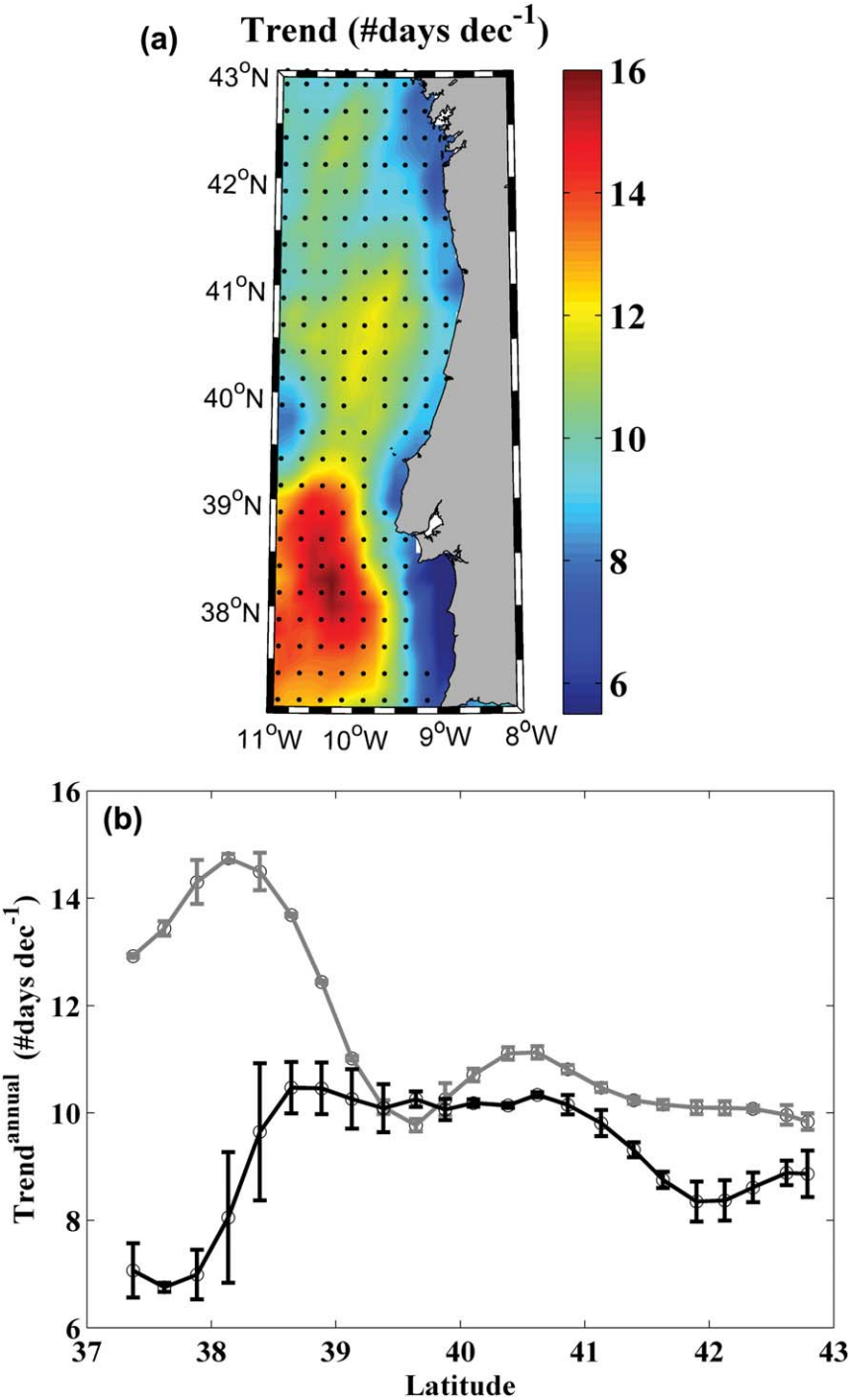


**Figure 2.** Annual trends in the number of extreme hot days (# days dec$^{-1}$) in the Atlantic Iberian sector over the period 1982–2012. (a) Map of trends. Dots mark trends with significance higher than 95%. (b) Trends at coastal (black line) and ocean (gray line) locations. Bars represent the standard deviation.

$$\sigma_{c_{i,j}}^2 = \frac{1}{n}\sum_{k,l}\left(\sigma_{i+k,j+l}^2 + \left({}^{95}\Delta N_{i+k,j+l} - \langle {}^{95}\Delta N_{i,j}\rangle\right)^2\right) \quad (1)$$

where ${}^{95}\Delta N_{i+k,j+l}$, $\sigma_{i+k,j+l}$, and $\sigma_{c_{i,j}}$ are the trend, the standard deviation, and the combined standard deviation in the neighborhood of pixel $i, j$; $n$ is the number of valid points in the neighborhood and $\langle {}^{95}\Delta N_{i,j}\rangle$ is the mean of all trends in that neighborhood. The subscripts $k$ and $l$ can only take the values −1, 0, and 1.

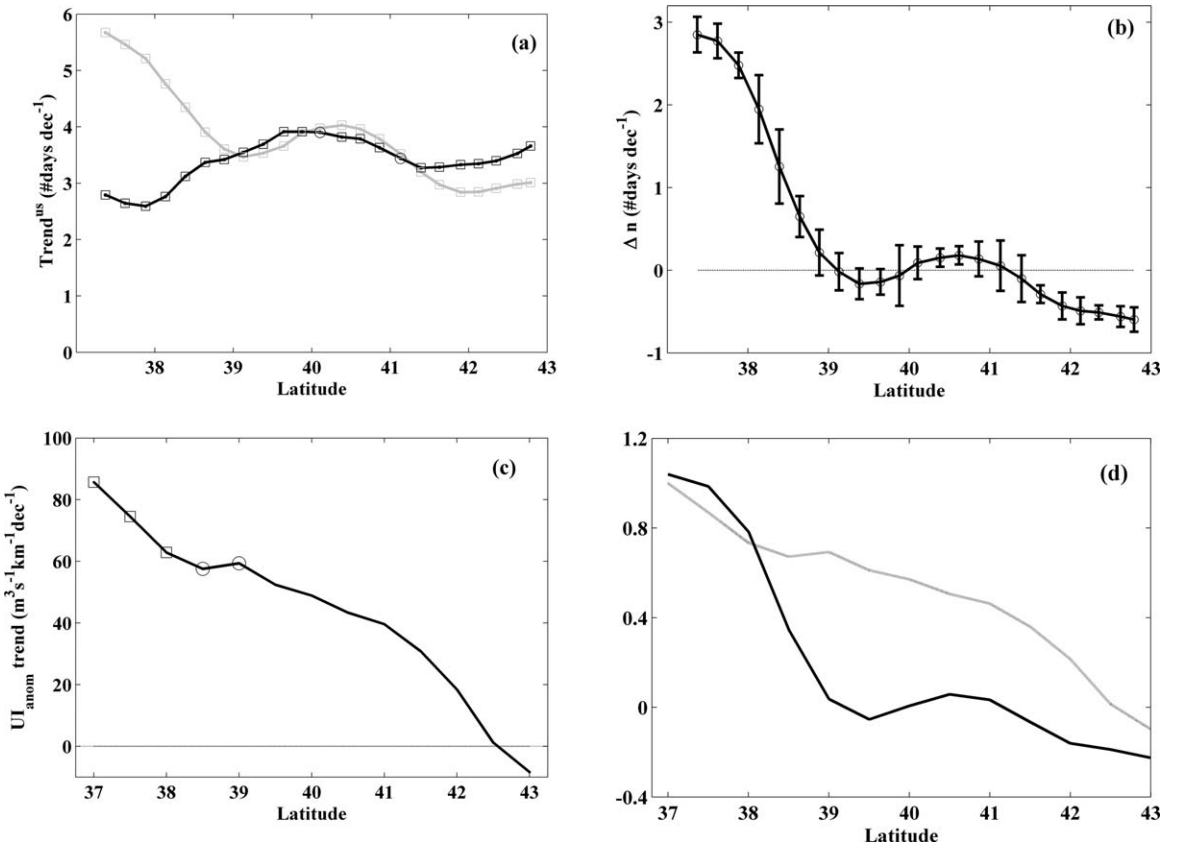


**Figure 3.** (a) Trends in the number of extreme hot days (# days dec$^{-1}$) near coast (black line) and at ocean locations (gray line) in the Atlantic Iberian sector during upwelling season (June–August) over the period 1982–2012. (b) Difference in the excess of extreme hot days between ocean and coastal locations (# days dec$^{-1}$). Bars represent the standard deviation. (c) Upwelling trends (m$^3$ s$^{-1}$ km$^{-1}$ dec$^{-1}$), during months with more intense upwelling (from June to August) in the Atlantic Iberian sector over the period 1982–2012. (d) Comparison between the signals previously depicted in Figures 3(b) and 3(c). Signals were normalized to improve visual comparison. In both Figures 3(b) and 3(c), circles mark trends with significance higher than 95% and squares trends with significance higher than 90%.

The maximum value of *n* is 9, but some of the pixels can be affected by land and then they must be discarded from the calculation. The same procedure was followed at seasonal scale. Note that extreme hot days are days whose anomaly in temperature is very high not its absolute temperature [*Lima and Wethey*, 2012].

The excess in extreme hot days was the variable chosen to characterize extremely hot events in the ocean. An extreme hot day is rarely isolated; these events usually last for a few days. In particular, the mean number of consecutive extreme hot days was 4.4 $\pm$ 5.8 (5.0 $\pm$ 7.4) days along the Atlantic Iberian sector (Moroccan subregion) from 1982 to 2012. This fact was not considered in the present analysis, where the number of extreme hot days per year (or per season) was calculated without taking into account whether an extreme hot day was isolated or not.

### 2.5. Upwelling Index

NCEP Climate Forecast System Reanalysis (CFSR) (http://rda.ucar.edu/pub/cfsr.html) is a wind product available at 6 hourly time resolution and 0.5° $\times$ 0.5° spatial resolution from January 1979 to December 2012, covering the atmosphere, ocean, sea ice, and land. CFSR database was developed by NOAA's National Centers for Environmental Prediction (NCEP). Data for the present study were retrieved from NOAA's National Operational Model Archive and Distribution System (NOMADS) which is maintained at NOAA's National Climatic Data Center (NCDC) [*Saha et al*., 2010]. Previous research carried out around the Iberian Peninsula [*Carvalho et al*., 2013; *Álvarez et al*., 2014], where different wind products were compared with in situ data provided by buoys, suggests that CFSR is an optimal choice in terms of accuracy, mesh fineness, length of the time series, and future data availability.

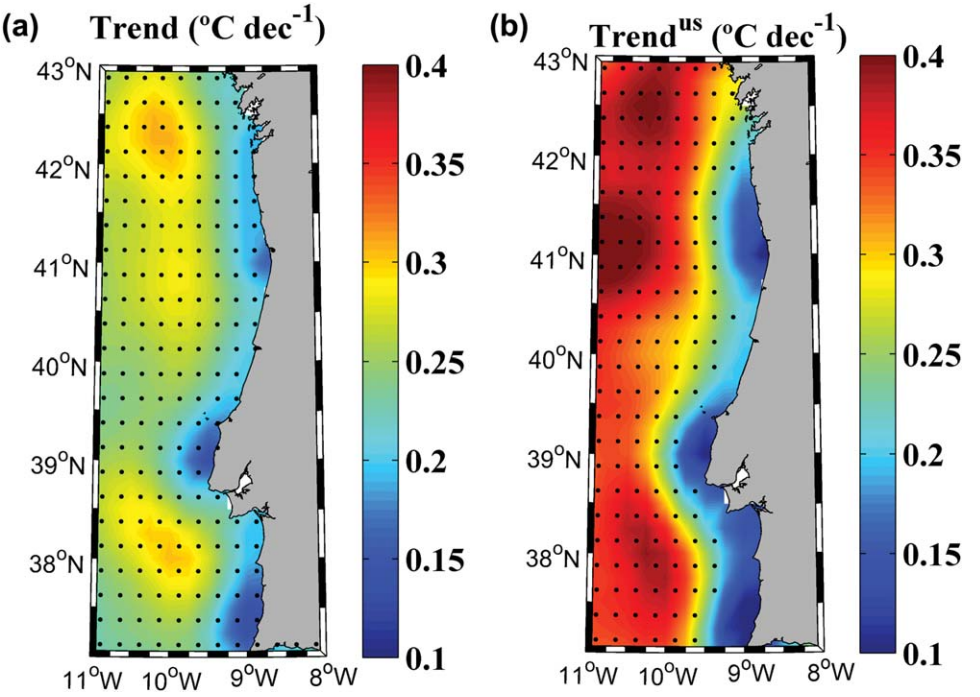


**Figure 4.** (a) Annual SST trends (°C dec$^{-1}$) and (b) trends during months with more intense upwelling (June–August), in the Atlantic Iberian sector over the period 1982–2012. Dots mark trends with significance higher than 95%.

Ekman transport was calculated following

$$Q_x = \frac{\rho_a C_d}{\rho f}\left(W_x^2 + W_y^2\right)^{1/2} W_y$$
$$Q_y = -\frac{\rho_a C_d}{\rho f}\left(W_x^2 + W_y^2\right)^{1/2} W_x \quad (2)$$

where W is the wind speed at a reference height of 10 m, $\rho$ is the sea water density (1025 kg m$^{-3}$), $C_d$ is a dimensionless drag coefficient ($1.4 \times 10^{-3}$), $\rho_a$ is the air density (1.22 kg m$^{-3}$), and $f$ is the Coriolis parameter defined as twice the vertical component of the Earth's angular velocity, $\Omega$, about the local vertical given by $f = 2\Omega\sin(\theta)$ at latitude $\theta$. Finally, x subscript corresponds to the zonal component and the y subscript to the meridional one.

Upwelling index (UI) can be defined as the Ekman transport component in the direction perpendicular to the shoreline [*Nykjaer and Van Camp*, 1994] following

$$UI = -\sin(\varphi)Q_x + \cos(\phi)Q_y \quad (3)$$

where $\varphi$ is the angle between the shore line and the equator (in average $\varphi = 90$ was considered for the Atlantic Iberian sector and $\varphi = 55$ for the Moroccan subregion). Positive (negative) upwelling indices correspond to upwelling-favorable (unfavorable) conditions. Six hourly wind data were converted to *UI* and then averaged at monthly scale. Finally, the linear trends of monthly anomalies were calculated over the period 1982–2011 for the points marked with crosses in Figure 1.

## 3. Results and Discussion

### 3.1. Atlantic Iberian Sector

Annual trends in the number of extreme hot days were calculated from 1982 to 2012 (Figure 2a). The number of extreme hot days has increased during this period with values ranging from 6 to 16 days dec$^{-1}$. The increase is not spatially homogeneous (Figure 2b) with higher trends at ocean (gray line) than at coastal locations (dark line). The excess in extreme hot days along the coast is similar to that obtained by *Lima and*

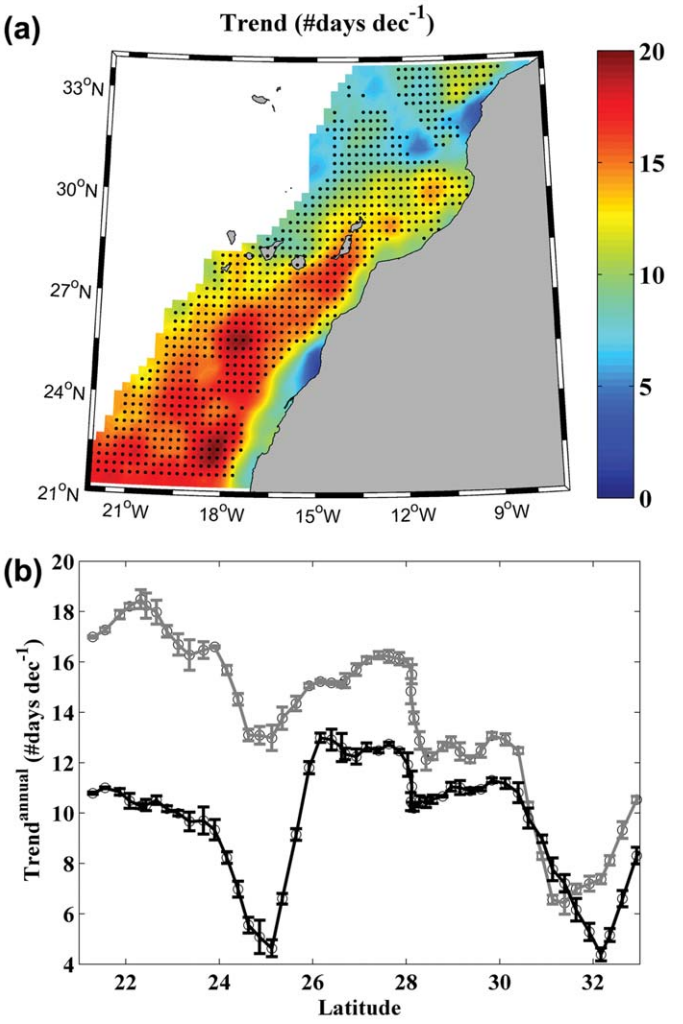


**Figure 5.** Annual trends in the number of extreme hot days (# days $dec^{-1}$) in the Moroccan subregion over the period 1982–2012. (a) Map of trends. Dots mark trends with significance higher than 95%. For the sake of clarity only the first six degrees from coast have been depicted. (b) Trends at coastal (black line) and ocean (gray line) locations. Bars represent the standard deviation.

*Wethey* [2012, region 4 in Figure 3b]. The lowest increase was detected near coast south of 39°N (black line) and the highest one at ocean locations for the same latitudes (gray line). The area south of 39°N shows the highest differences between coast and ocean at annual scale. North of 39°N, these differences are practically negligible, although the increase in the number of hot days tends to be slightly larger for ocean locations. Only around 42°N the difference increases again, although at a much lesser extent than observed south of 39°N.

Previous research mentioned the existence of different warming rates at coastal and ocean waters in the Atlantic Iberian sector [*Relvas et al*., 2009; *Santos et al*., 2011a, 2012a]. In spite of these studies mentioned the possible role played by upwelling on coastal warming, this effect was not quantified. Two mechanisms can be responsible of the different warming rates at coastal and adjacent ocean locations. First, the presence of upwelling enhances the vertical advection and prevents the diffusion of temperature from surface as suggested in *Santos et al*. [2012a]. Second, upwelling reinforcement can result in increasing the amount of cold water that is pumped from deeper layers to the surface, which also slows down the coastal heating induced by global warming. This mechanism was previously described for other upwelling regions [*Santos et al*., 2012b, 2012c]. These previous studies have motivated the analysis of extreme hot days over the period June to August, upwelling season from now on (Figure 3). Actually, upwelling extends from April to September, but only the months under the most intense upwelling conditions have been considered. The number of extreme hot days increases at all ocean locations (Figure 3a, gray line), being larger at low latitudes (approximately 6 days $dec^{-1}$ at 37°N) than at high latitudes (approximately 3 days $dec^{-1}$ at 43°N). In contrast, the number of extreme hot days also increases near coast (black line) ranging from 3 to 4 days $dec^{-1}$. The variable $\Delta n = \Delta n^o - \Delta n^c$ (# days $dec^{-1}$) is defined as the difference between the increment in the number of extreme hot days at the ocean ($\Delta n^o$) and at the coast ($\Delta n^c$). The highest $\Delta n$ values are observed south of 39°N being almost negligible for the rest of the latitudes and even negative north of 41°N (Figure 3b). A significant positive upwelling trend (ranging from 60 and 90 $m^3\ s^{-1}\ km^{-1}\ dec^{-1}$) is observed south of 39°N during upwelling season (Figure 3c). For the rest of the latitudes, coastal upwelling trend decreases with latitude and it becomes no significant north of 39°N and even negative north of 42°N. The signals in plots b and c were normalized (divided by the maximum value of each signal) to be represented together (Figure 3d). Apart from the visual resemblance between signals the Spearman correlation

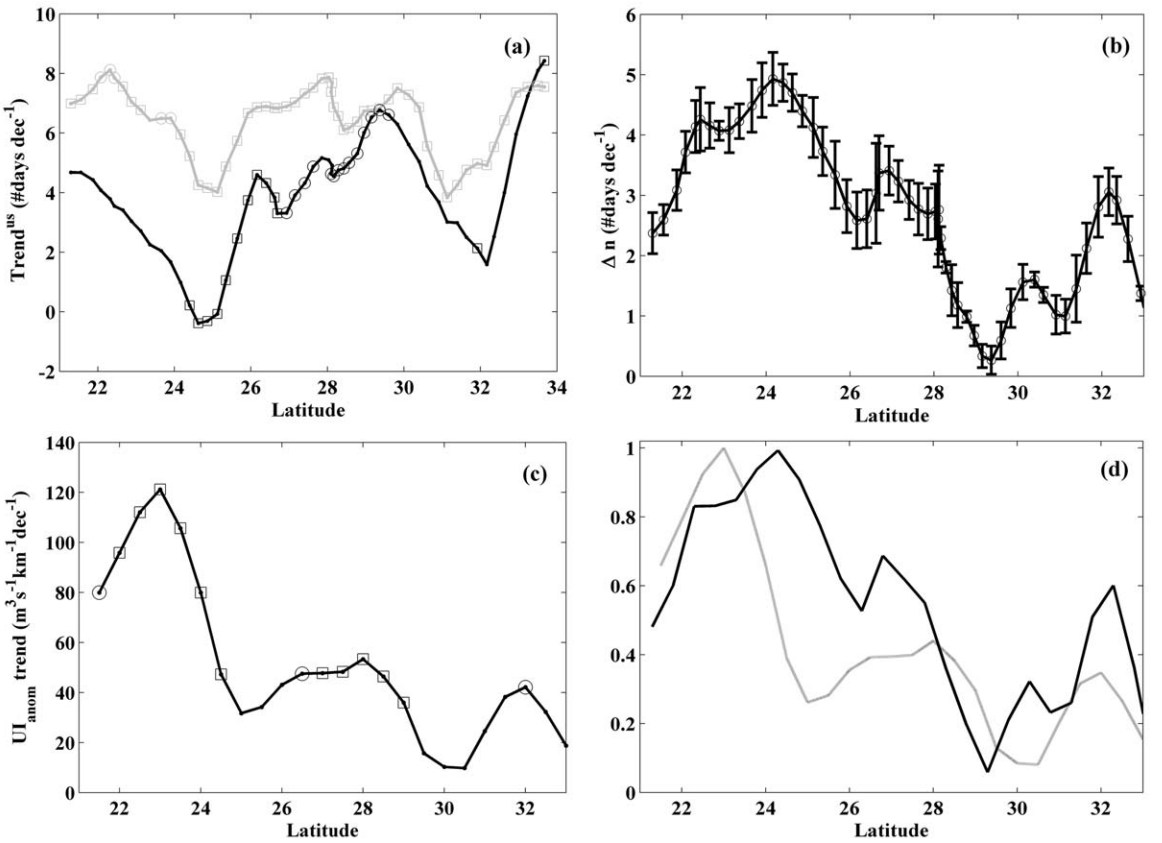


**Figure 6.** (a) Trends in the number of extreme hot days (# days dec$^{-1}$) near coast (black line) and at ocean locations (gray line) in the Moroccan subregion during upwelling season (April–September) over the period 1982–2012. (b) Difference in the excess of extreme hot days between ocean and coastal locations (# days dec$^{-1}$). Bars represent the standard deviation. (c) Upwelling trends (m$^3$ s$^{-1}$ km$^{-1}$ dec$^{-1}$), during months with more intense upwelling (April–September), in the Moroccan subregion over the period 1982–2012. (d) Comparison between the signals previously depicted in Figures 6(b) and 6(c). Signals were normalized to improve visual comparison. In both Figures 6(a) and 6(c), circles mark trends with significance higher than 95% and squares trends with significance higher than 90%.

among them is significant (R = 0.88, $p < 0.01$). Actually, Δn is large for areas where positive coastal upwelling trends are also large.

For comparison purposes, Figure 4 shows the SST trend calculated over the period 1982–2012 both at annual scale and during the upwelling season (June–August). Remarkable differences in warming trends can be observed between coast and ocean. Annual coastal warming (Figure 4a) is similar to that detected by *Lima and Wethey* [2012] for the Southwest European coast (∼0.2–0.3°C dec$^{-1}$) over the period 1985–2005. In addition, the patterns are consistent with those shown by *Relvas et al*. [2009] and with changes in the number of extreme hot events shown in Figures 2 and 3.

### 3.2. Moroccan Subregion

Annual trends in the number of extreme hot days were also calculated along the Moroccan subregion (Figure 5a) over the period 1982–2012. For the sake of clarity only the first six degrees from coast will be depicted in the maps corresponding to the Moroccan area. The number of extreme hot days has increased during this period with values ranging from <5 to 19 days dec$^{-1}$. The increase is not spatially homogeneous (Figure 5b). Overall, trends tend to be higher at ocean (gray line) than at coastal locations (black line) with local minima trends in extreme hot days at 25°N and 32°N. The excess in extreme hot days along the coast is similar to that obtained by *Lima and Wethey* [2012, regions 5 and 6 in Figure 3b]. Differences between coast and ocean are higher south of 27°N (∼8 days dec$^{-1}$) and practically negligible north of 31°N (1–2 days dec$^{-1}$), although the increase in extreme hot days tends to be slightly larger for ocean locations. Between 27°N and 31°N, the differences between coast and ocean exist (2–4 days dec$^{-1}$) but they are not so intense as south of 27°N probably due to the presence of the Canary archipelago.

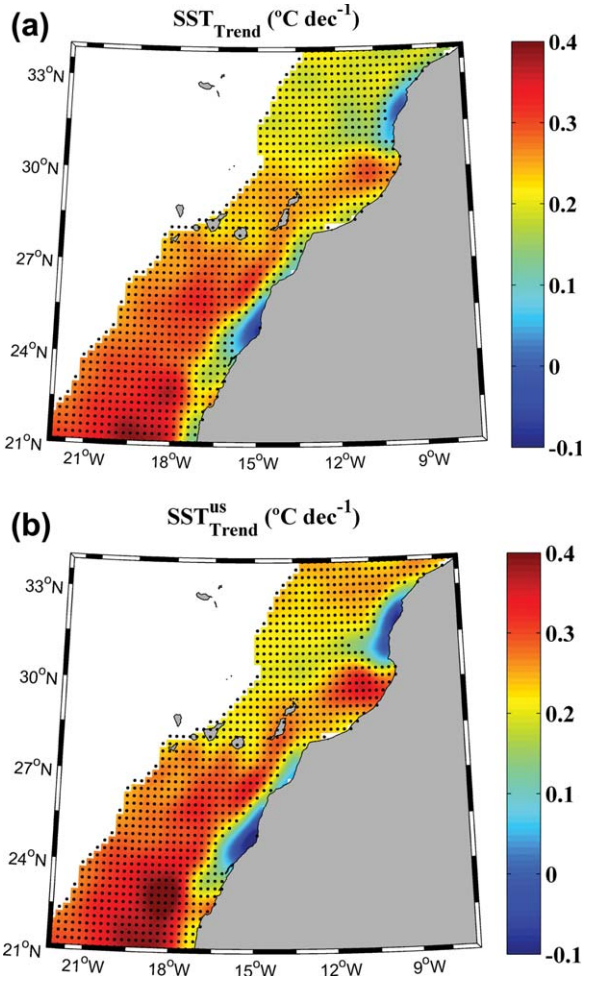


**Figure 7.** (a) Annual SST trends (°C dec$^{-1}$) and (b) during months with more intense upwelling (April–September), in the Moroccan subregion over the period 1982–2012. Dots mark trends with significance higher than 95%.

An analysis of trends in extreme hot days during the upwelling season is depicted in Figure 6. Although upwelling can be observed all over the year, only the months under the most intense upwelling conditions (April–September) have been considered, upwelling season from now on. First of all, the excess in the number of extreme hot days follows a similar pattern both near coast and at ocean locations, although values are higher at ocean locations (gray line) than near coast (black line) for all latitudes (Figure 6a). According to the variable $\Delta n = \Delta n^o - \Delta n^c$ (# days dec$^{-1}$) defined above, the highest values for the Moroccan region (Figure 6b) are observed south of 28°N (between 2 and 5 days dec$^{-1}$) and at 32°N (3 days dec$^{-1}$). $\Delta n$ becomes practically negligible between 28°N and 31°N which are the latitudes influenced by the Canary archipelago. These results are consistent with the previous studies [*Santos et al.*, 2012c] in which the highest differences in SST trends between coast and ocean were obtained south of 28°N and around 32°N. As for coastal upwelling (Figure 6c), trends are positive during the upwelling season for the whole Moroccan subarea being especially intense south of 24°N, with values ranging from 50 to 120 m$^3$ s$^{-1}$ km$^{-1}$ dec$^{-1}$, and near 32°N with values around 50 m$^3$ s$^{-1}$ km$^{-1}$ dec$^{-1}$. As previously done for Figure 3, the signals in plots b and c were normalized to be represented together (Figure 6d). Once again, apart from the visual resemblance between signals the Spearman correlation among them is significant ($R = 0.67$, $p < 0.01$).

Figure 7 shows the annual and upwelling season SST trends calculated over the period 1982 to 2012 for comparison purposes. Annual coastal warming (Figure 7a) is similar to that detected by *Lima and Wethey* [2012] in Northwest Africa for the region dominated by the Canary current (0.1–0.2°C dec$^{-1}$) for the period 1985–2005. In addition, these patterns are consistent with changes in the number of extreme hot events shown in Figures 5 and 6.

## 4. Conclusions

SST warming observed in previous studies for the Canary upwelling ecosystem is reflected in changes in the number of extreme hot events. The main findings of the present study can be summarized as follows:

1. The annual number of extreme hot days has increased along the Atlantic Iberian sector and the Moroccan subregion of the CUE over the period 1982–2012.

2. The excess in extreme hot days is lower near coast than at adjacent ocean locations.

3. The difference in the excess of extreme hot days between ocean and coastal locations is particularly evident for months under strong upwelling conditions (JJA in the Atlantic Iberian sector and AMJJAS in the Moroccan subregion).

4. The highest differences in the excess of extreme hot days between coastal and ocean locations ($\Delta$n (# days dec$^{-1}$)) occur at those regions where coastal upwelling increase is high. Actually, $\Delta$n and upwelling trends have shown to be significantly correlated in both areas, R = 0.88 ($p < 0.01$) at the Atlantic Iberian sector and R = 0.67 ($p < 0.01$) at the Moroccan subregion.

In summary, upwelling seems to be the local mechanism that mitigates the increase in the number of extreme hot days near coast both for the Atlantic Iberian sector and the Moroccan subregion.

**Acknowledgments**
This work was partially supported by Programa de Consolidación e Estruturación de Unidades de Investigación (Grupos de Referencia Competitiva) funded by European Regional Development Fund (FEDER) and by Xunta de Galicia under project 10PXIB383169PR and cofunded by the European Regional Development Fund (FEDER). NOAA OI1/4 Degree Daily SST data were provided by NOAA's National Climatic data Center. NCEP Climate Forecast System Reanalysis (CFSR) (http://rda.ucar.edu/pub/cfsr.html) was developed by NOAA's National Centers for Environmental Prediction (NCEP).

## References

Álvarez, I., M. Gómez-Gesteira, M. deCastro, and J. M. Dias (2008), Spatiotemporal evolution of upwelling regime along the western coast of the Iberian Peninsula, *J. Geophys. Res.*, *113*, C07020, doi:10.1029/2008JC004744.

Álvarez, I., M. Gomez-Gesteira, M. deCastro, and D. Carvalho (2014), Comparison of different wind products and buoy wind data with seasonality and interannual climate variability in the southern Bay of Biscay (2000–2009), *Deep Sea Res., Part II*, doi:10.1016/j.dsr2.2013.09.028, in press.

Arístegui, J., E. D. Barton, X. A. Álvarez-Salgado, A. M. P. Santos, F. G. Figueiras, S. Kifani, S. Hernández-León, E. Mason, E. Machú, and H. Demarcq (2009), Sub-regional ecosystem variability in the Canary Current upwelling, *Prog. Oceanogr.*, *83*(1–4), 33–48, doi:10.1016/j.pocean.2009.07.031.

Barriopedro, D., E. M. Fischer, J. Luterbacher, R. M. Trigo, and R. García-Herrera (2011), The hot summer of 2010: Redrawing the temperature record map of Europe, *Science*, *332*, 220–224, doi:10.1126/science.1201224.

Barton, E. D., D. B. Field, and C. Roy (2013), Canary current upwelling: More or less?, *Prog. Oceanogr.*, *116*, 167–178, doi:10.1016/j.pocean.2012.07.007.

Belkin, I. M. (2009), Rapid warming of large marine ecosystems, *Prog. Oceanogr.*, *81*, 207–213, doi:10.1016/j.pocean.2009.04.011.

Burrows, M. T., et al. (2011), The pace of shifting climate in marine and terrestrial ecosystems, *Science*, *334*, 652–655, doi:10.1126/science.1210288.

Carvalho, D., A. Rocha, M. Gómez-Gesteira, I. Alvarez, and C. Silva Santos (2013), Comparison between CCMP, QuikSCAT and buoy winds along the Iberian Peninsula coast, *Remote Sens. Environ.*, *137*, 173–183, doi:10.1016/j.rse.2013.06.005.

Cheung, W. W. L., R. Watson, and D. Pauly (2013), Signature of ocean warming in global fisheries catch, *Nature*, *497*, 365–369, doi:10.1038/nature12156.

Cropper, T. E., E. Hanna, and G. R. Bigg (2014), Spatial and temporal seasonal trends in coastal upwelling off Northwest Africa, 1981–2012, *Deep Sea Reasearch 1*(86), 94–111, doi: 10.1016/j.dsr2014.01.007.

deCastro, M., M. Gomez-Gesteira, A. M. Ramos, I. Álvarez, and P. deCastro (2011), Effects of heat waves on human mortality, Galicia, Spain, *Clim. Res.*, *48*, 333–341, doi:10.3354/cr00988.

Dessai, S. (2002), Heat stress and mortality in Lisbon. Part I: Model construction and validation, *Int. J. Biometeorol.*, *47*, 6–12, doi:10.1007/s00484-002-0143-1.

Díaz, J., R. Garcia-Herrera, R. M. Trigo, C. Linares, M. A. Valente, J. M. De Miguel, and E. Hernandez (2006), The impact of summer 2003 heat wave in Iberia: How should we measure it?, *Int. J. Biometeorol.*, *50*(3), 159–166, doi:10.1007/s00484-005-0005-8.

Diederich, S., G. Nehls, J. E. E. van Beusekom, and K. Reise (2005), Introduced Pacific oyster (*Crassostrea gigas*) in the northern Wadden Sea: Invasion accelerated by warm summers?, *Helgoland Mar. Res.*, *59*, 97–106, doi:10.1007/s10152-004-0195-1.

Frank, K. T., B. Petrie, J. S. Choi, and W. C. Leggete (2005), Trophic cascades in a formerly cod-dominated ecosystem, *Science*, *308*, 1621–1623, doi:10.1126/science.1113075.

García-Herrera, R., J. Diaz, R. M. Trigo, and E. Hernandez (2005), Extreme summer temperatures in Iberia: Health impacts and associated synoptic conditions, *Ann. Geophys.*, *23*, 239–251, doi:10.5194/angeo-23-239-2005.

Gómez-Gesteira, M., M. deCastro, I. Álvarez, and J. L. Gómez-Gesteira (2008a), Coastal sea surface temperature warming trend along the continental part of Atlantic Arc (1985–2005), *J. Geophys. Res.*, *113*, C04010, doi:10.1029/2007JC004315.

Gómez-Gesteira, M., M. deCastro, I. Álvarez, M. N. Lorenzo, J. L. G. Gesteira, and A. J. C. Crespo (2008b), Spatio-temporal Upwelling trends along the canary upwelling system (1967–2006), trends and directions in climate research, *Ann. N. Y. Acad. Sci.*, *1146*, 320–337, doi:10.1196/annals.1446.004.

Gómez-Gesteira, M., et al. (2011), The state of Climate in North-West Iberia, *Clim. Res.*, *48*, 109–144, doi:10.3354/cr00967.

Honkoop, P. J. C., J. Van der Meer, J. J. Beukema, and D. Kwast (1998), Does temperature-influenced egg production predict the recruitment in the bivalve *Macoma balthica*?, *Mar. Ecol. Prog. Ser.*, *64*, 229–235.

Kostianoy, A. G., and A. G. Zatsepin (1996), The West African coastal upwelling filaments and cross-frontal water exchange conditioned by them, *J. Mar. Syst.*, *7*, 349–359, doi:10.1016/0924-7963(95)00029-1.

Lemos, R. T., and H. O. Pires (2004), The upwelling regime off the west Portuguese coast, 1941–2000, *Int. J. Climatol.*, *24*, 511–524, doi:10.1002/joc.1009.

Lemos, R. T., and H. O. Sansó (2006), Spatio-temporal variability of ocean temperature in the Portugal Current System, *J. Geophys. Res.*, *111*, C04010, doi:10.1029/2005JC003051.

Lima, F. P., and D. S. Wethey (2012), Three decades of high-resolution coastal sea surface temperatures reveal more than warming, *Nat. Commun.*, *3*, 704, doi:10.1038/ncomms1713.

Lima, E. P., N. Queiroz, P. A. Ribeiro, S. J. Hawkins, and A. M. Santos (2006), Recent changes in the distribution of a marine gastropod, *Patella rustica Linnaeus*, 1758, and their relationship to unusual climate events, *J. Biogeogr.*, *33*, 812–822, doi:10.1111/j.1365-2699.2006.01457.x.

Lima, E. P., P. A. Ribeiro, N. Queiroz, S. J. Hawkins, and A. M. Santos (2007), Do distributional shifts of northern and southern species of algae match the warming pattern?, *Change Biol.*, *13*, 2592–2604, doi:10.1111/j.1365-2486.2007.01451.x.

McGregor, H., M. Dima, H. Fischer, and S. Mulitza (2007), Rapid 20th-century increase in coastal upwelling off northwest Africa, *Science*, *315*, 637–639, doi:10.1126/science.1134839.

Nykjaer, L., and L. Van Camp (1994), Seasonal and Interannual variability of coastal upwelling along northwest Africa and Portugal from 1981 to 1991, *J. Geophys. Res.*, *99*, 14,197–14,207, doi:10.1029/94JC00814.

Occhipinti-Ambrogi, A. (2007), Global change and marine communities: Alien species and climate change, *Mar. Pollut. Bull.*, *55*, 342–352, doi:10.1016/j.marpolbul.2006.11.014.

Pardo, P. C., X. A. Padín, M. Gilcoto, L. Farina-Busto, and F. F. Pérez (2011), Evolution of upwelling systems coupled to the long-term variability in sea surface temperature and Ekman transport, *Clim. Res.*, *48*, 231–246, doi:10.3354/cr00989.

Pauly, D., and V., Christensen (1995), Primary production required to sustain global fisheries, *Nature*, *374*, 255.

Philippart, C. J. M., H. van Aken, J. J. Beukema, O. G. Bos, G. C. Cadeé, and R. Dekker (2003), Climate-related changes in recruitment of the bivalve Macoma balthica, *Limnol. Oceanogr.*, *48*(6), 2171–2185.

Press, W. H., S. A. Teukolsky, W. T. Vetterling, and B. P. Flannery (1992), *Numerical Recipes in C. The Art of Scientific Computing*, 2nd ed., Cambridge Univ. Press, Cambridge, U. K.

Quenouille, M. H. (1952), *Associated Measurements*, 242 pp., Butterworths, London, U. K.

Relvas, P., J. Luís, and A. M. P. Santos (2009), Importance of the mesoscale in the decadal changes observed in the northern Canary upwelling system, *Geophys. Res. Lett.*, *36*, L22601, doi:10.1029/2009GL040504.

Reynolds, R. W. (2009), What's new in Version 2. [Available at http//www.ncdc.noaa.gov/oa/climate/research/sst/papers/whats_new_v2.pdf.]

Reynolds, R. W., and D. W. Chelton (2010), Comparisons of daily sea surface temperature analysis for 2007–08, *J. Clim.*, *23*, 3545–3562, doi:10.1175/2010JCLI3294.

Saha, S., et al. (2010), The NCEP Climate Forecast System Reanalysis, *Bull. Am. Meteorol. Soc.*, *91*, 1015–1057, doi:10.1175/2010BAMS3001.1.

Santos, A. M. P., A. S. Kazmin, and A. Peliz (2005), Decadal changes in the Canary upwelling system as revealed by satellite observations: Their impact on productivity, *J. Mar. Res.*, *63*, 359–379, doi:10.1357/0022240053693671.

Santos, F., M. Gómez-Gesteira, and M. deCastro (2011a), Coastal and Oceanic SST variability along the western Iberian Peninsula, *Cont. Shelf Res.*, *31*, 2012–2017, doi:10.1016/j.csr.2011.10.005.

Santos, F., M. Gómez-Gesteira, M. deCastro, and I. Álvarez (2011b), Upwelling along the western coast of the Iberian Peninsula: Dependence of trends on fitting strategy, *Clim. Res.*, *48*, 213–218, doi:10.3354/cr00972.

Santos, F., M. Gómez-Gesteira, M. deCastro, and I. Álvarez (2012a), Variability of coastal and ocean water temperature in the upper 700 m along the Western Iberian Peninsula from 1975 to 2006, *PLoS One*, *7*(12), 1–7, doi:10.1371/journalpone.0050666.

Santos, F., M. Gómez-Gesteira, M. deCastro, and I. Álvarez (2012b), Differences in coastal and oceanic SST trends due to the strengthening of coastal upwelling along the Benguela current system, *Cont. Shelf Res.*, *34*, 79–86, doi:10.1016/j.csr.2011.12.004.

Santos, F., M. deCastro, M. Gomez-Gesteira, and I. Álvarez (2012c), Differences in coastal and oceanic SST warming rates along the Canary upwelling ecosystem from 1982 to 2010, *Cont. Shelf Res.*, *47*, 1–6, doi:10.1016/j.csr.2012.07.023.

Thieltges, D. W. (2006), Parasite induced summer mortality in the cockle *Cerastoderma edule* by the trematode Gymnophallus choledochus, *Hydrobiologia*, *559*(1), 455–461, doi:10.1007/s10750-005-1345-4.

Trigo, R. M., A. M. Ramos, P. J. Nogueira, F. D. Santos, R. Garcia-Herrera, C. Gouveia, and F. E. Santo (2009), Evaluating the impact of extreme temperature based indices in the 2003 heatwave excessive mortality in Portugal, *Environ. Sci. Policy*, *12*, 844–854, doi:10.1016/j.envsci.2009.07.007.

Wethey, D. S., et al. (2011), Response of intertidal populations to climate: Effects of extreme events versus long term change, *J. Exp. Mar. Biol. Ecol.*, *400*, 132–144, doi:10.1016/j.jembe.2011.02.008.